npj | climate and atmospheric science

Article

Published in partnership with CECCR at King Abdulaziz University

https://doi.org/10.1038/s41612-024-00700-7

Occurrence of an unusual extensive ice-free feature within the pack ice of the central Weddell Sea, Antarctica

Babula Jena [1] ✉, John Turner[2], Tylei Reeves-Francois[2], C. C Bajish [3], Caroline Holmes[2], Thomas Caton Harrison[2], Tony Phillips [2] & Zhaomin Wang[4]

We investigate an unusual extensive ice-free feature (EIF) within the pack ice that developed in the central Weddell Sea in December 1980 on the edge of the multi-year sea ice off the east coast of the Antarctic Peninsula. The EIF was first apparent on satellite imagery on 8 December 1980 and expanded until it reached its largest areal extent of ~5.4×10^5 km^2 on 26 December. The combined influences of near-record strength (~ 15 ms^{-1}) cold winds from the Antarctic continent (transporting sea ice northward and creating an area of thin ice), increased shortwave radiation and net heat flux into the ocean, passage of deep polar storms, and the upwelling of high saline warm water led to the opening of this unique EIF. It is still the largest ice-free feature within the pack ice resembling a polynya observed in the central Weddell Sea during the satellite era, contributing significantly to the 1981 Weddell Sea sea ice extent minimum of 0.793×10^6 km^2, the lowest on record. The development mechanism of this EIF was different from the 1970's Weddell open ocean polynya which occurred within the winter sea ice cover through enhanced ocean convection.

Polynyas are largely ice-free areas within the main sea ice zone that are important features of the Southern Ocean[1–4]. A number of different types of polynyas have been observed over recent decades. They develop as coastal polynyas[5], or deep within the ice pack as open-ocean polynyas[6] that can be observed at any time of the year. The extensive ice-free area within the pack ice resembling a polynya described in this paper developed during the period of sea ice retreat in the early summer (Figs. 1a–d and 2). We have referred to it as an extensive ice-free feature (EIF) as it differs in formation mechanism from classical winter polynyas but still satisfies broader definitions used in many scholarly works[7–11]. Polynyas have a significant impact on ocean deep water formation[12], with winter polynyas being responsible for the production of Antarctic Bottom Water, which is the densest water mass in the ocean. They also have an effect on local and regional atmospheric circulation patterns through changes in net heat fluxes[13], and can lead to anomalously low sea ice extent (SIE) at the following annual minimum in late summer[14,15]. Polynyas are important to the ocean environment because of the transformation of water masses through ocean cooling, atmospheric CO_2 absorption, and the large ocean-atmosphere moisture and heat fluxes associated with them[16].

Since early satellite measurements began in the 1970's, there have been a number of polynyas, several of which developed in the Weddell Sea. The most studied has been the 'Weddell polynya', which appeared during the winters of 1974, 1975 and 1976[1], forming as a result of enhanced open ocean convection and the upwelling of high salinity warm Weddell deep water (Fig. 3). Other major polynyas have formed intermittently close to Maud Rise at 66 °S, 3 °E[17] and north of the edge of the Ronne Ice Shelf[18]. Open ocean polynyas such as those found in the Cosmonaut[2] and Cooperation Seas[19] have also been observed persistently to the east of the Weddell Sea.

A number of theories have been proposed to explain the occurrence of polynyas based on observational and modelling studies. Polynyas are typically classified as either 'sensible heat' or 'latent heat'. 'Sensible heat' polynyas are thermally driven, and associated with changes in ocean convection and mixing. They are also known as 'open ocean' polynyas and are maintained through sensible heating by warm upwelling waters. 'Latent heat' polynyas are more dynamically driven. Also known as 'coastal polynyas', they form as a result of near-surface winds transporting ice away from a region, and are maintained through latent heating as the cold exposed ocean surface refreezes[20,21]. Atmosphere-ocean interactions are important in the occurrence and intensity of polynyas[13], with ocean preconditioning and meteorological perturbations both being crucial[22]. Storm activity, atmospheric rivers, warm air advection[23], and water column stability fluctuations[1] are crucial factors in polynya formation and these are known to be linked

[1]National Centre for Polar and Ocean Research, Ministry of Earth Sciences, Goa, India. [2]British Antarctic Survey, Natural Environment Research Council, Cambridge, UK. [3]KSCSTE - Institute for Climate Change Studies, Kottayam, India. [4]Southern Marine Science and Engineering Guangdong Laboratory (Zhuhai), Zhuhai, China. ✉e-mail: bjena@ncpor.res.in

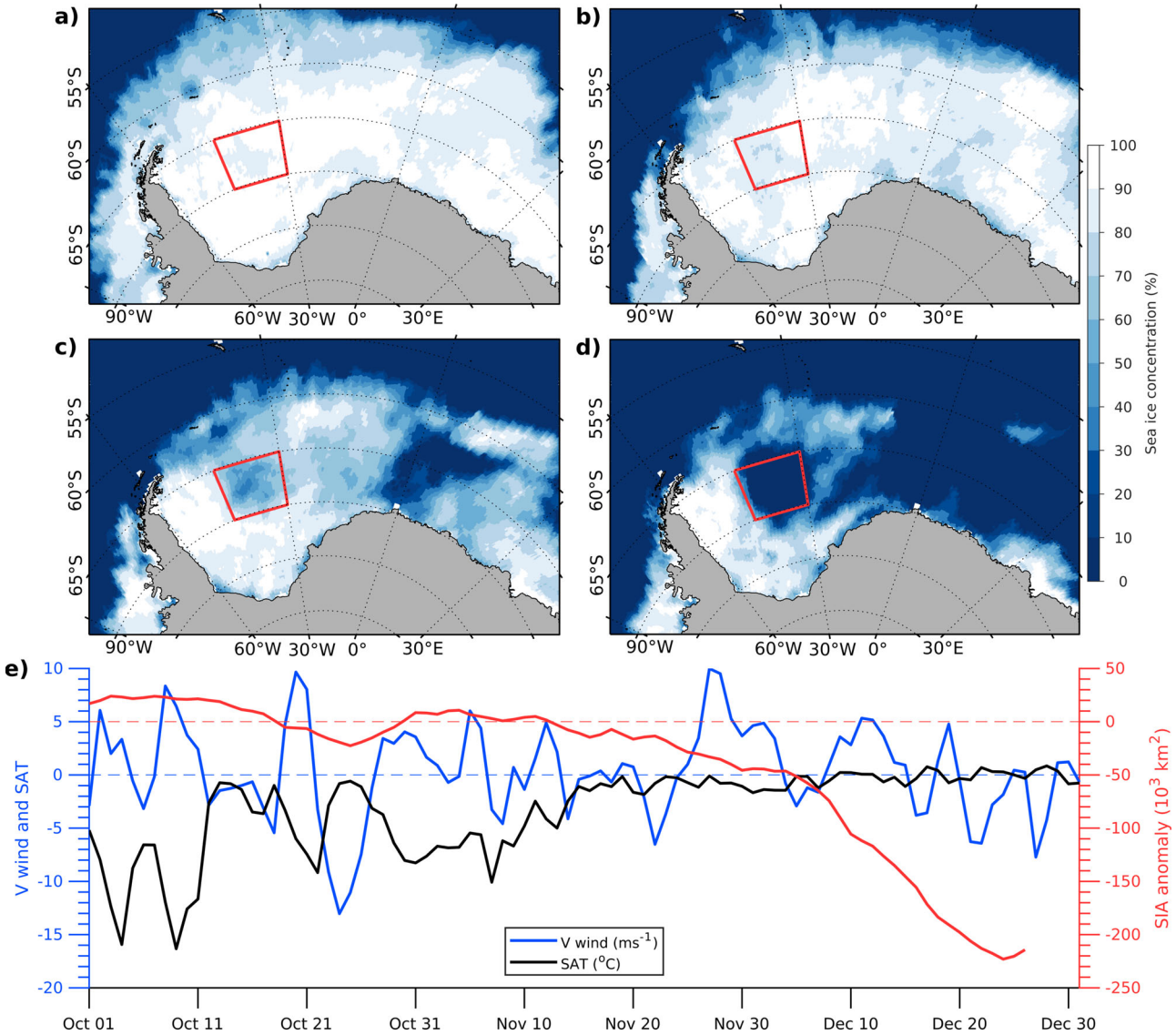

Fig. 1 | The evolution of sea ice in the Weddell Sea in late 1980 illustrating the development of the extensive ice-free feature (EIF). The sea ice concentration (SIC) fields are shown for (**a**) 24 September when the sea ice extent (SIE) was at its annual maximum, **b** 8 November, when strong westerly winds advected sea ice away from the multi-year ice creating a distinct low SIC area that subsequently expanded and became the EIF, **c** 6 December, when the central Weddell Sea EIF was first apparent as a distinct feature on the satellite imagery, and **d** 26 December, when the EIF was at its greatest extent. The EIF box is outlined in red. **e** The 1 October–31 December daily mean sea ice area (SIA) anomaly, mean 10 m V wind and the maximum 2 m surface air temperature (SAT) in the EIF box.

with the various modes of climate variability[22–26]. Studies using coupled climate models have determined that the build-up of a subsurface heat reservoir was important in the opening of the Weddell Polynya, alongside deep ocean convection[27,28]. The strengthening of Weddell gyre played an important role for the occurrence of the Weddell Sea polynya during the 1970's[28]. Development of polynyas in the austral spring/summer is strongly influenced by the ice-albedo feedback because of the seasonal increase in solar radiation[29–31]; this in turn has an influence on the sea ice concentration (SIC) at the minimum several months later. In the southern part of the Weddell Sea the Ronne Polynya is a near-perennial feature that is a result of the strong climatological southerly winds flowing off the Ronne Ice Shelf. In 1997 the polynya was particularly extensive as a result of El Niño forcing[5], which had promoted anomalously strong southerly near-surface winds. The highest production of sea ice in the Weddell Sea occurs in the Ronne Polynya[32], but a heat reservoir is required alongside convective mixing for the polynya to survive the freezing winter[22]. Development of the Cosmonaut Sea Polynya has been attributed to vertical water column stretching resulting in the upwelling of warmer saline water into the surface layer[2]. Formation of the Maud Rise Polynya has been attributed to a combination of negative wind stress curl, large cyclonic eddies and seamount interaction (upwelling of high saline-warm water), and advection of warm air from mid-latitudes causing a ~ 11.5°C temperature increase led to ice melt in September 2017[17,23]. It is important to note that the Weddell Sea polynya in the 1970's[1] usually formed as an extension of the Maud Rise Polynya (Fig. 3).

Here we examine the development of the previously undocumented open ocean EIF that developed in the central Weddell Sea in December 1980 on the edge of the multi-year sea ice off the east coast of the Antarctic Peninsula. This development was unique in two ways; the event was not influenced by the Maud Rise polynya and also did not develop by deep ocean convection during winter. The EIF was first apparent in satellite imagery on 8 December 1980 at 68°S, 40°W and it expanded until 26 December when it covered an area of 5.4×10^5 km^2, just before the edge of the EIF was breached. It is still the largest ice free feature within the pack ice to have occurred in the central Weddell Sea in the satellite era.

This paper is organised as follows. The following section describes the atmospheric and oceanic environment before the EIF developed, and how

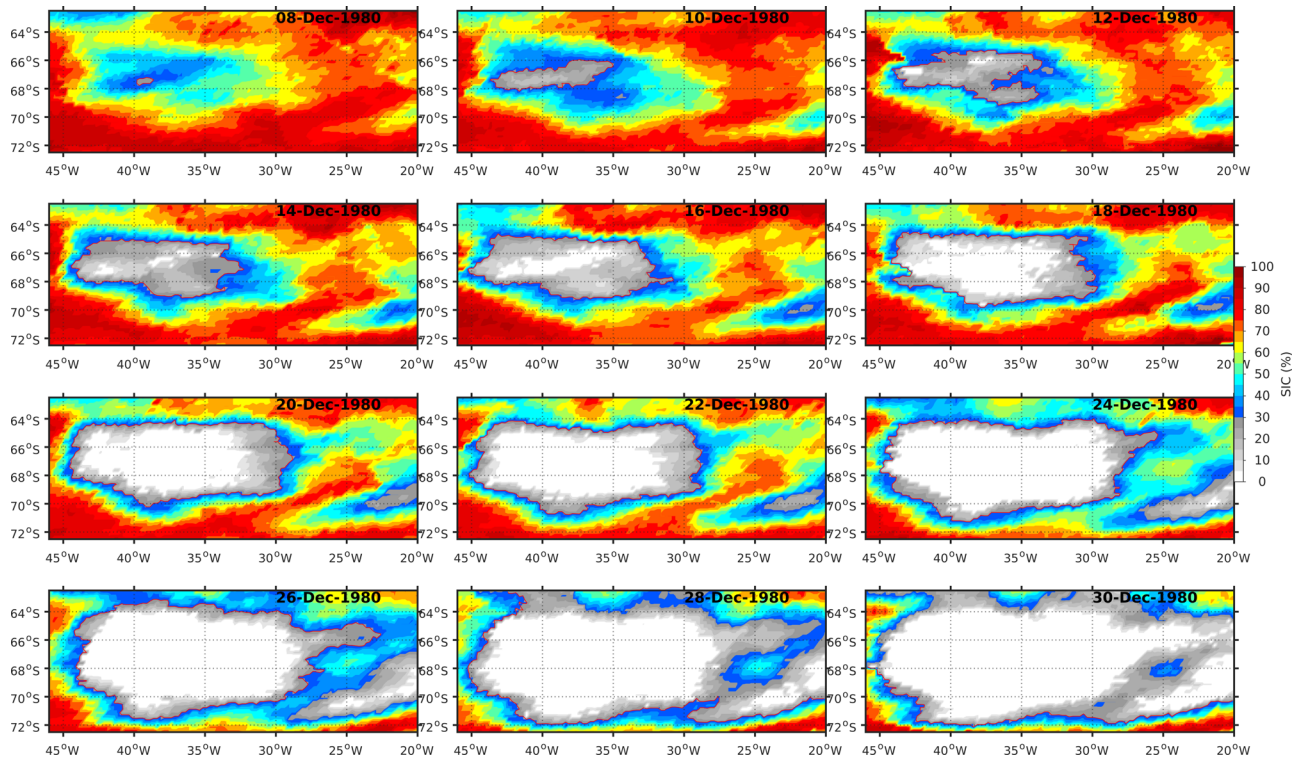

Fig. 2 | The evolution of extensive ice-free feature (EIF). The EIF from 8 to 30 December 1980 as seen in the sea ice concentration (SIC) derived from the satellite passive microwave imagery. The boundary of the EIF is taken as SIC > 30% and is shown by the red line.

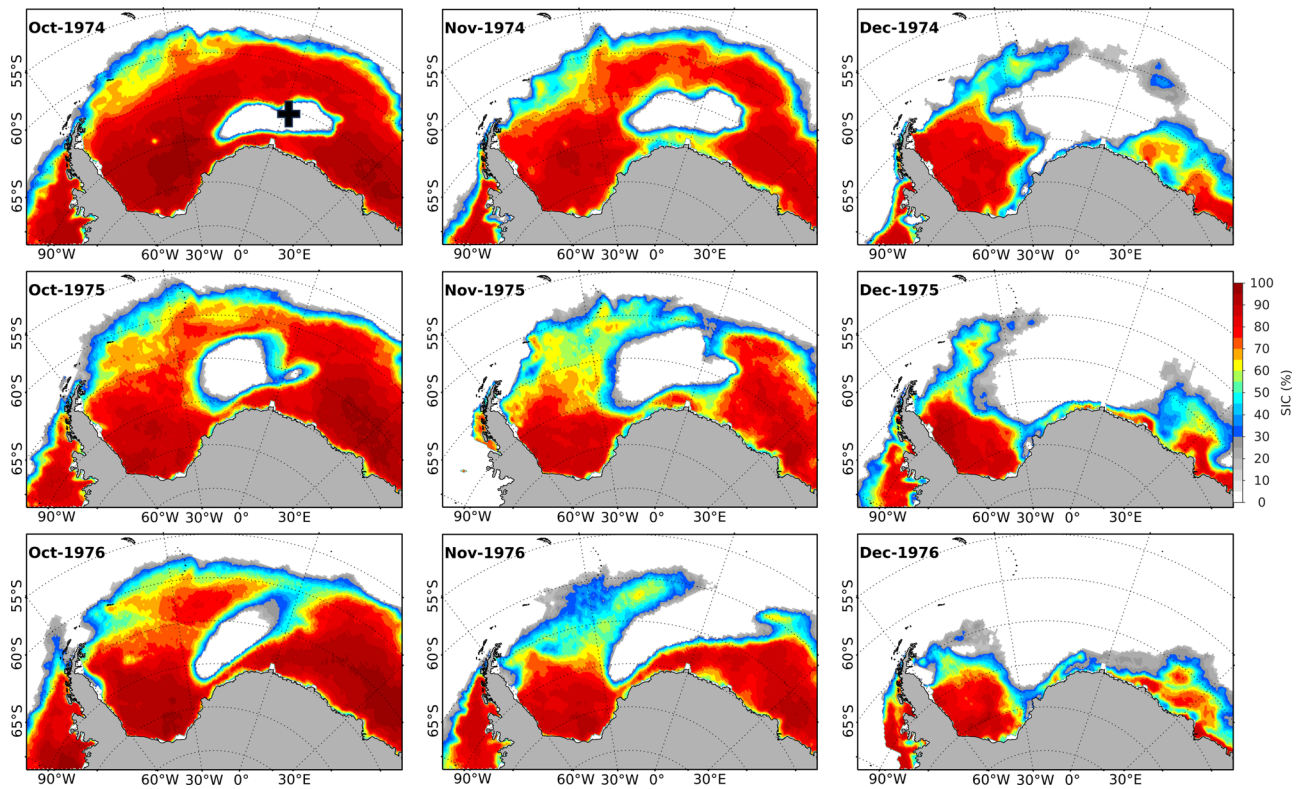

Fig. 3 | The Weddell Sea polynya in 1970's. Observations of the Weddell Sea polynya from the Nimbus-5 Electrically Scanning Microwave Radiometer (ESMR). The black cross mark shows the location of the Maud Rise.

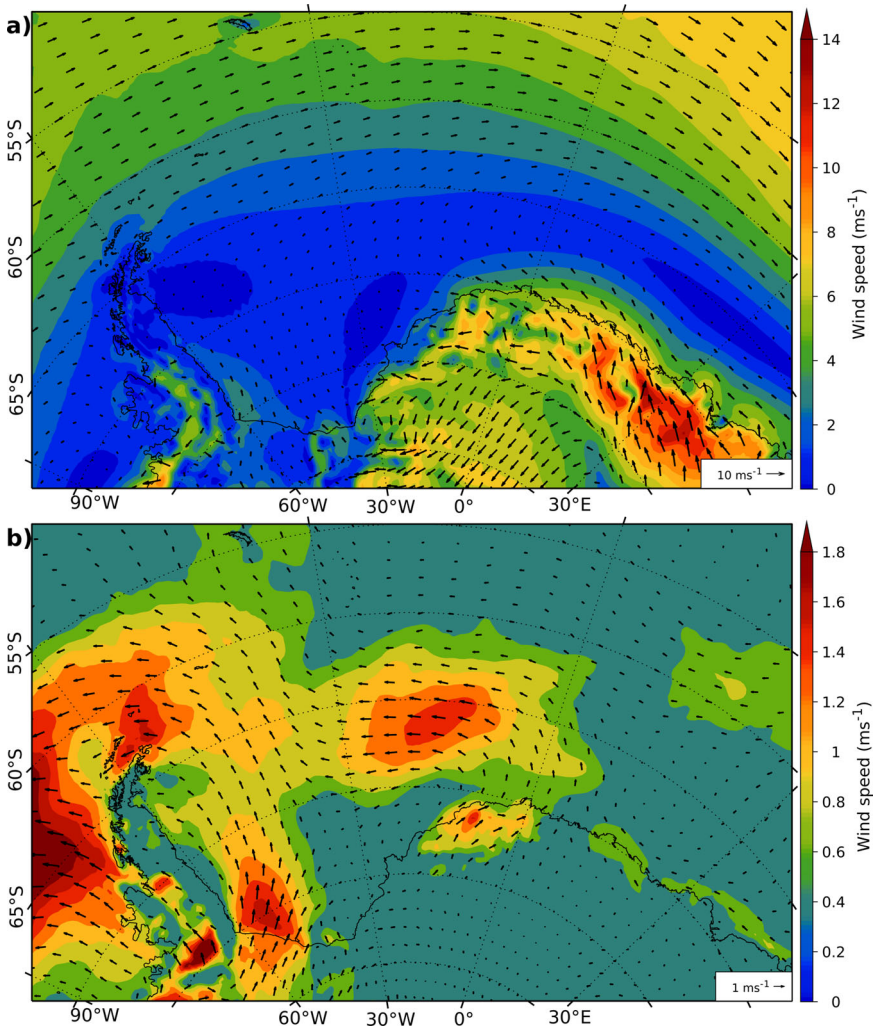

Fig. 4 | Anomalously strong southerly winds creating an extensive area of thin ice prior to formation of the extensive ice-free feature (EIF). **a** The climatological wind field (at 10 m) over the Weddell Sea, **b** wind speed anomalies for January–October 1980.

the ice cover evolved up to the subsequent annual sea ice minimum. Subsequent sections present a summary and discuss future work needed. The last section presents the data and methods used.

Results

Conditions prior to formation of the open ocean EIF

Sea ice conditions in 1979 were not exceptional, with no indication of a polynya or significant area of low SIC in the central Weddell Sea, suggesting that the ocean/sea ice environment the previous year had little impact on the opening of the EIF in December 1980. Instead, the EIF developed as a result of air–sea conditions in the months leading up to the austral summer of 1980/81.

Climatologically, the Weddell Sea is dominated by cyclonic atmospheric and oceanic circulations around the basin (the Weddell Gyre) and strong westerly winds to the north (Fig. 4a), both of which play a key part in the evolution of the sea ice. During January–October 1980 there were particularly strong southerly winds over the western Weddell Sea, with the 10 m meridional wind speed anomaly being >1 m s^{-1} over an extensive area (Fig. 4b). The strong southerlies were a result of anomalously low pressure over the eastern Weddell Sea and high pressure over the Antarctic Peninsula. The 10 m meridional wind speed anomaly was >1.5 m s^{-1} north of the Ronne Ice Shelf and >1 m s^{-1} over the latitude/longitude area 65°−70°S, 45°−30°W, which broadly covers the area of the EIF at its maximum extent on 26 December 1980 (Fig. 1d), and is referred to subsequently as the 'EIF box'. The mean April–September 1980 meridional wind speed in the EIF box was 2.2 m s^{-1}, which was the strongest in the record, with mean meridional winds of 15 m s^{-1} on 25 June 1980 the highest daily value in the whole record post 1979. The July monthly mean meridional wind speed was 3.6 m s^{-1}, which was also the strongest in the 43-year record. These exceptional southerly winds resulted in anomalously high sea ice advection towards the north, with the Weddell Sea SIE of 7.8 × 10^6 km^2 on 24 September 1980 (Fig. 1a) being the highest annual maximum in the record. The advection of sea ice northwards opened leads within the pack ice that refroze, creating new thin ice, in a similar way to what takes place just north of the Ronne Ice Shelf[18]. Although the sea ice area (SIA) in the box had a positive anomaly at the start of October (Fig. 1e), the fact that it was relatively thin ice made it susceptible to melt from intrusions of warm air and upwelling of warm sub-surface water masses from below.

During October 1980, a succession of deep storms developed in the Weddell Sea bringing anomalously warm air into the sea ice zone on their eastern flank and advecting sea ice northwards as they moved towards the east. The atmospheric conditions during the month were variable, with alternating episodes of northerly and southerly near-surface flow (Fig. 1e), with the maximum 2 m air temperature within the box varying between 0.6 °C and −17.5 °C.

The first significant October storm developed over the western Weddell Sea over 13/14 October and was the first of a series of lows that formed in the lee of the Antarctic Peninsula. The low then deepened rapidly and drew warm air from the north (Figs. 5a and 6). The maximum 2 m air temperature in the EIF box rose from −13.8 °C at 06 UTC 11 October to 0.3 °C at 18 UTC 14 October, leading to limited sea ice melt. A further lee cyclone developed on 17 October and deepened rapidly as it tracked slowly

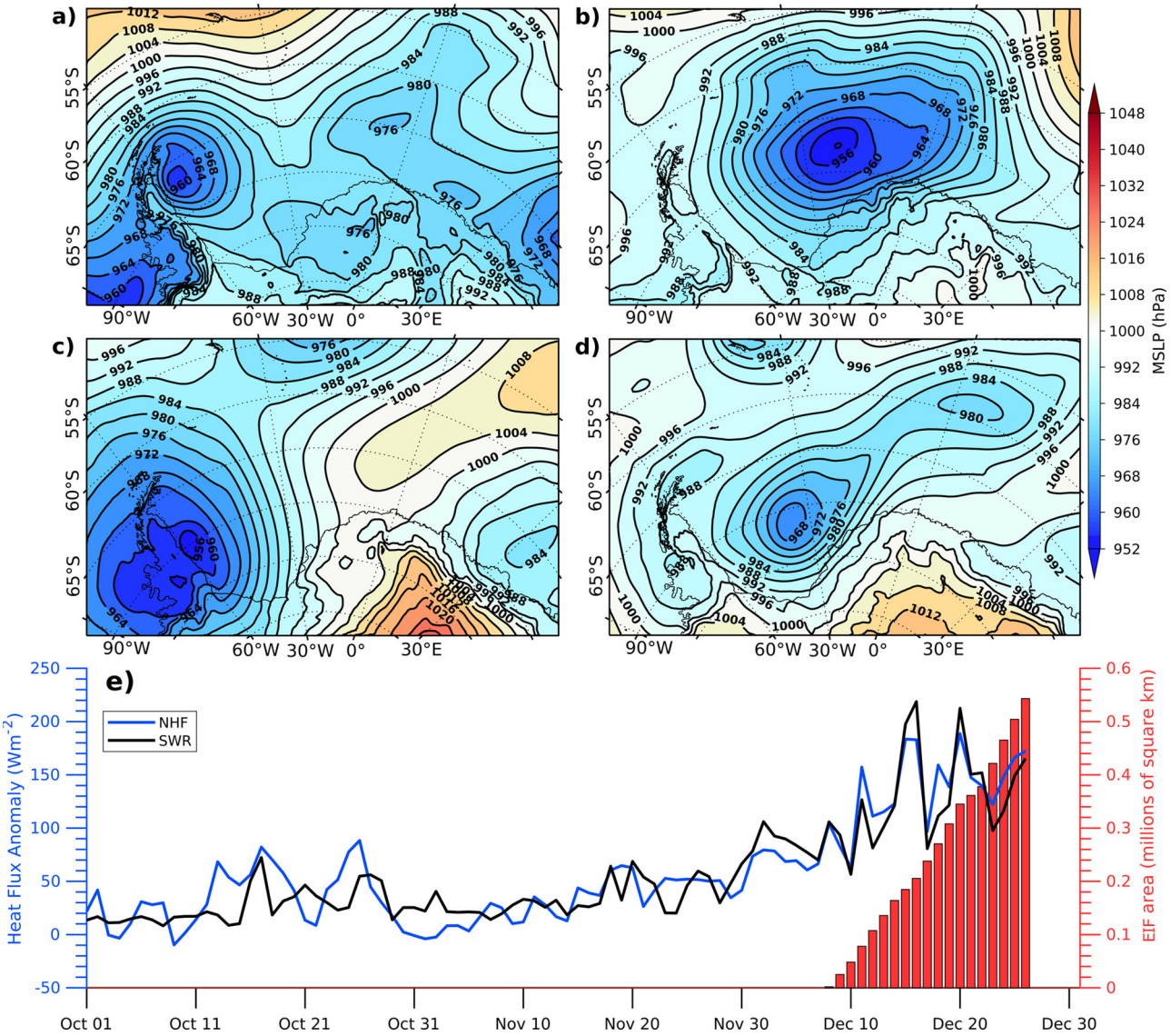

Fig. 5 | Polar storms and their impact on the formation of the extensive ice-free feature (EIF). The mean sea level pressure (hPa) for (**a**) 18 UTC 14 October 1980, **b** 00 UTC 19 October 1980, **c** 18 UTC 25 October and **d** 18 UTC 6 November. **e** The daily shortwave radiation (SWR), net heat flux (NHF) and the area of the central Weddell Sea EIF covering 1 October–31 December 1980.

eastwards over the following few days (Fig. 5b). It gave mean southerly winds of 9.7 ms^{-1} over the EIF box on 20 October that led to export of sea ice northwards and a subsequent decrease of SIA in the EIF box (Fig. 1e). Following the period of cold southerly flow, a third lee cyclogenesis event took place on 24 October in the southwest Weddell Sea and there was another northerly wind episode, with the wind speed being even stronger than on 14 October (Fig. 5a). This storm extended across most of the Antarctic Peninsula (Fig. 5c) and the warm air intrusion occurred as a narrow band of high temperature air extending from the north (Fig. 6b). The maximum near-surface temperature was 0.6 °C at 18 UTC 25 October, which was within the top 2.5% of October temperatures in the EIF box, indicating the exceptional nature of the warm air intrusion into the area. However, with temperatures only just above freezing, sea ice melt probably contributed little to the SIA anomaly of -22×10^3 km^2 on 25 October (Fig. 1e), which was mainly a result of sea ice advected out of the region in the earlier strong southerly flow.

The impact of the storms on the sea ice was considerable, with the SIA within the box decreasing by 42,000 km^2 between 11 and 25 October. During this period the shortwave radiation and net heat flux anomaly within the box was positive, reaching a maximum of 90 W m^{-2} on 24 October (Fig. 5e).

Following the strong northerly winds on 24/25 October the winds reverted to a more climatological southerly flow and near-surface temperatures dropped below freezing, with temperatures of close to −7 °C until ~12 November (Fig. 1e). Between 4 and 7 November a depression tracked from near the tip of the Antarctic Peninsula to the southern Weddell Sea (Fig. 5d) leading to strong (> 10 m/s) westerly winds north of the low centre, which advected first year sea ice away from the edge of the multi-year sea ice on the western side of the Weddell Sea. The mean zonal wind in the EIF box was 8.7 ms^{-1} on 7 November, and though not particularly anomalous, these were the strongest westerly winds since spring. The westerly winds led to a decrease in SIC (Fig. 1b) and marked the start of a near-linear decline in the SIA in the box leading up to the appearance of the EIF on 8 December (Fig. 1e).

The climatological average ocean conditions in the EIF box during October–November consist of a low saline cold water mass near the surface with a mixed layer depth (MLD) of ~50 m separated from an underlying high saline dense water mass (Supplementary Fig. 1a, b). In the vicinity of the EIF, domed isopycnals are evident with downward slopes to the north and south of the EIF box. This condition is conducive to further uplift of the isopycnals towards the surface with favourable atmospheric wind flow

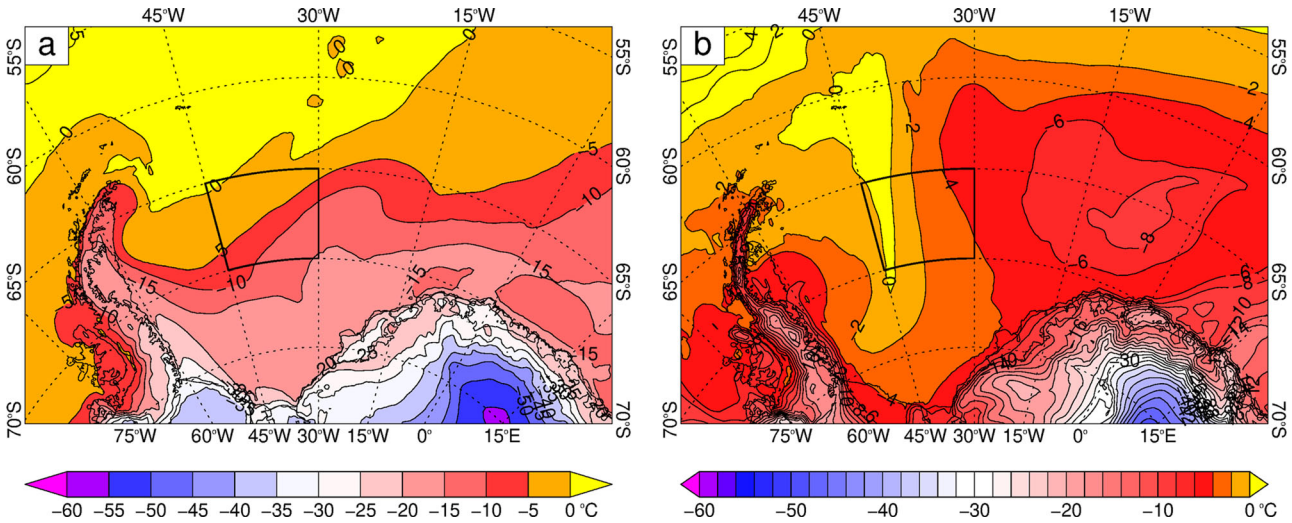

Fig. 6 | Intrusion of warm air from the mid-latitudes. The ECMWF ERA5 based 2 m air temperature on (**a**) 18 UTC 14 October 1980 and (**b**) 18 UTC 25 October 1980. The extensive ice-free feature (EIF) box is outlined in black.

(negative wind stress curl) and internal ocean dynamics (localised convection). During November-December 1980, the denser isopycnals ($\sigma_\theta \geq 27.7$) reached the surface (Supplementary Fig. 1c, d) with an anomalous warming of up to ~1°C and high saline-dense water mass (~ 0.3 psu, ~0.25 kg m^{-3}) in the mixed layer indicating upwelling of water masses from below the mixed layer (Fig. 7). The wind stress conditions in the Weddell Sea modulate the observed isopycnal layers and are known to intensify the strength of the Weddell Sea gyre, thus controlling the upwelling and downwelling of water masses[27,33]. On synoptic timescales, the strong wind stress associated with polar storms lifts the sub-surface warm circumpolar deep-water towards the surface, limiting sea ice growth or promoting ice melting. During November 1980 there was an anomalously negative wind stress curl of up to -2.2×10^{-7} N m^{-3} at the surface with a distinct cyclonic circulation in the central Weddell Sea (Fig. 7a) that strengthened the Weddell gyre[28,34]. This circulation pattern was favourable for the upwelling of unusually warm and high saline-dense water towards the surface, resulting in ice thinning. Apart from the thermodynamic impact on sea ice, the dynamic effect, specifically the strengthening of the Weddell Gyre leading to divergence within its inner section, also contributed to the thinning of ice due to ice divergence. However, the wind stress curl during this period was not unprecedented in the context of the time series of data from 1979 to 2021.

Formation and expansion of the open ocean EIF

During November 1980, there was a steady decline in the SIA within the EIF box as a result of ice melt caused by the upwelling of warm sub-surface waters, ice divergence and the increasing shortwave radiation during the month, with the loss of thin sea ice amplified by the ice-albedo feedback. There was also a period of strong (> 10 m/s) southerly winds over 27–28 November that advected more sea ice to the north (Fig. 1e). However, the most rapid SIA decline began after the EIF was first apparent as a clearly defined feature in the satellite data on 8 December (Figs. 1c and 2), when it had an area of 1929 km^2 as determined from the area where the SIC was >30%. After 8 December, the shortwave radiation and net heat flux in the box grew substantially, albeit with large daily variability (Fig. 5e).

During December a number of depressions crossed the Weddell Sea giving alternating northerly and southerly winds (Fig. 1e), but the meridional wind pattern was not correlated with the SIA in the box, which declined steadily, suggesting that the ice-albedo feedback was responsible for the dramatic expansion of the EIF during the month at a time when there was a maximum in the incoming solar radiation.

The vertical cross section (depth vs. time) of potential temperature and MLD spatially averaged over the EIF box shows a shallow mixed layer (< 25 m) with anomalously high temperatures (> 1 °C) in December 1980 (Supplementary Fig. 2). The warming of the mixed layer was associated with the anomalous large net heat flux (> 100 W m^{-2}) during the formation of the EIF (Fig. 5e).

The SIE for the whole Weddell Sea sector (Supplementary Fig. 3) had a large positive anomaly in September 1980 as a result of the anomalously strong southerly flow. However, the SIE declined rapidly during December, with the anomaly switching from positive to negative on 25 December. The decline occurred not only because of the development of the central Weddell Sea EIF, but because of the reoccurrence of the Maud Rise polynya further to the east. This was first identifiable on 22 November close to 69 °S, 5 °E, before it extended northwards and came into contact with the ice edge on 10 December when its existence as a polynya ended. The EIF and Maud Rise polynya therefore coexisted for a short period, but together contributed significantly to the large negative SIE anomaly for the Weddell Sea sector, with the 1981 annual SIE minimum being 0.793×10^6 km^2 on 5 March, which was the record lowest in the satellite era. In February 1981, the Weddell Sea experienced exceptionally low sea ice conditions, with SIE at the fourth lowest (0.889×10^6 km^2) and SIA at the lowest ever (0.594×10^6 km^2) levels in the satellite era.

Discussion

The development of the central Weddell Sea EIF in December 1980 was different from that of the Maud Rise polynyas, and also from the 1970's Weddell Sea polynya which formed with a huge ice-free region in the main ice pack and remains a unique occurrence within the 43-year passive microwave satellite data record. The SIA in the central Weddell Sea in late spring and early summer has varied over the decades and there have been years of more extensive leads and occasions when the ice edge intruded into the EIF box, but there has not been any other occasion when a low SIC area expanded into a major EIF.

This inter-annual variability of the ice cover in the central Weddell Sea can be appreciated from the time series of SIA in the EIF box on 26 December over 1979–2021 (Supplementary Fig. 4). While the minimum SIA in the EIF box in the record was 22,295 km^2 in 1980, the second lowest was 73,969 km^2 in 2001. On this occasion the low SIA was not the result of a polynya but a very southerly sea ice edge that had been forced south by anomalously strong northeasterly winds. The third lowest SIA in the box was 83,386 km^2 in 1982, one year after the development of the major feature considered here. With a very extensive area of open water in the central Weddell Sea in December 1980 and during the months leading up to the annual sea ice minimum, the ocean warmed in late 1980 and early 1981 when the incoming shortwave solar radiation was at its maximum (Fig. 5e).

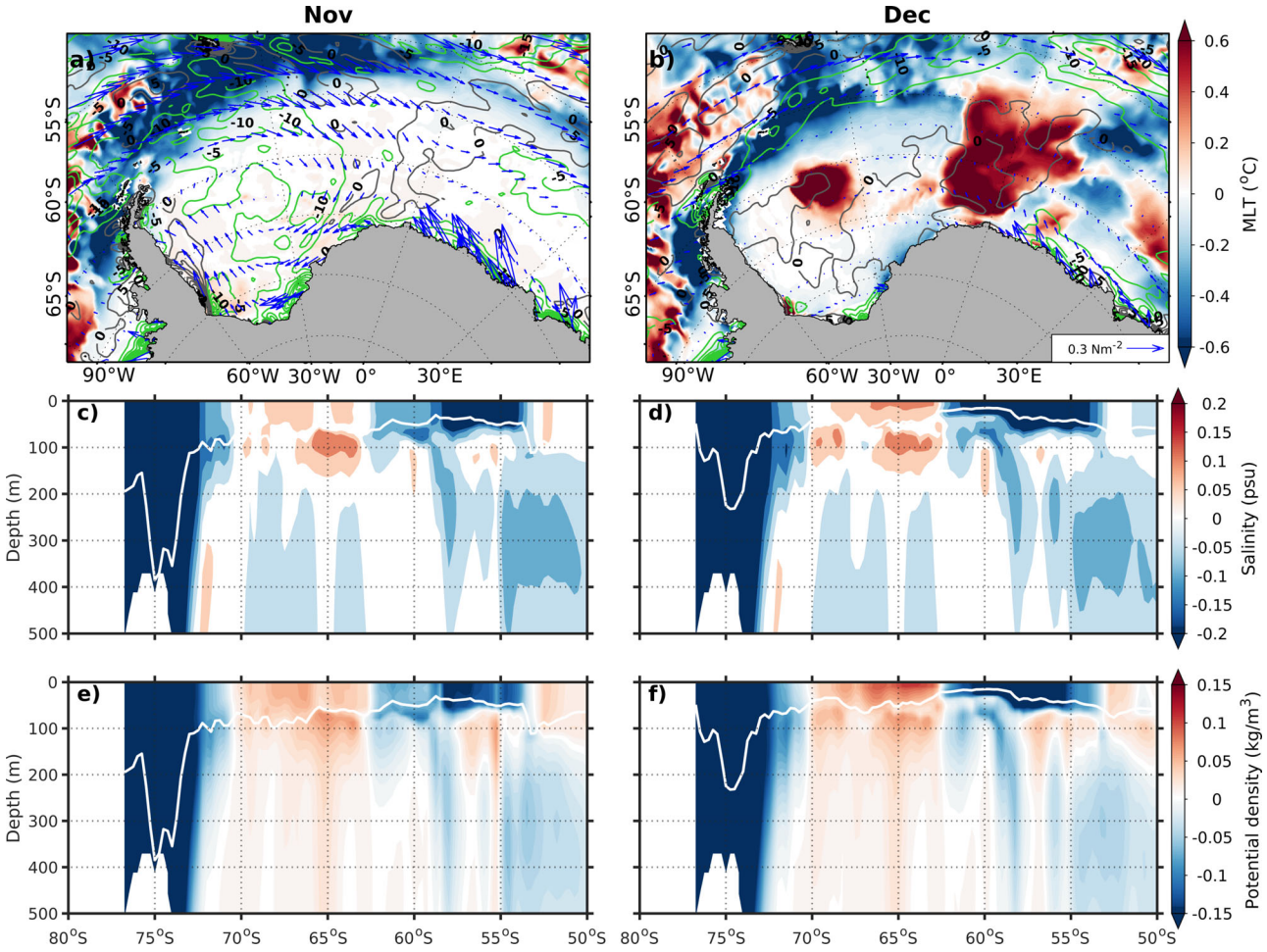

Fig. 7 | Upper-ocean changes during occurrence of the extensive ice-free feature (EIF). Anomalies in (**a**) and (**b**) ocean mixed layer temperature (MLT), wind stress vectors (blue arrows), negative wind stress curl (green contours, N m^{-3}) and positive wind stress curl (grey contours) during November–December 1980 from the long-term mean (1979–2008). Depth-Latitude cross section of the ECMWF ORAS5 based (**c**, **d**) salinity and (**e**, **f**) potential density anomaly along 40°W (passing through the EIF) during November–December 1980. White lines indicate the variability in mixed layer depth.

The high temperatures in the mixed layer persisted into late 1981 and were well represented by the ocean reanalysis (Supplementary Fig. 2). The relatively high mixed layer temperatures led to an early sea ice decline in November 1981, which was similar to that of late 1980. However, the early sea ice decline was also influenced by the development of a small polynya off the coast of the eastern Weddell Sea and the low ice concentrations extending southwards from the ice edge over the northern Weddell Sea. As the central Weddell Sea EIF did not reappear in late 1981 there was no repeat of the very rapid sea ice decline seen in 1980 (Supplementary Fig. 5).

We cannot quantify the relative importance of the various atmospheric and oceanic factors that led to development of the 1980 EIF using the available data. However, it seems likely that several factors played a part in triggering the initial appearance of the EIF, which then grew rapidly in a non-linear fashion as a result of the ice-albedo feedback. One of the most important factors was the occurrence of strong southerly winds ahead of the annual SIA maximum. The mean April–September meridional wind speed over the EIF box in 1980 was the strongest in the record and the advection of large amounts of sea ice to the north with the opening of leads that re-froze, creating new thin ice was clearly an important factor in preconditioning the region for subsequent rapid ice melt.

Other years of strong southerly winds did not see the development of an EIF. For example, in 1988 the April–September meridional wind speed over the box was only slightly less than in 1980, but 1988 lacked the strong westerly flow off the multi-year sea ice that occurred in November 1980 that the satellite imagery shows preceded the opening of the EIF. The marked negative wind stress curl over the EIF area in October also did not occur in 1988.

To summarise, the EIF developed close to the edge of the multi-year sea ice following near-record strength (~ 15 ms^{-1}) southerly winds during April-September 1980. Ice was advected northwards creating leads that re-froze in the cold southerly flow, with the new thin ice susceptible to rapid melt. Sea ice loss occurred through gain of shortwave radiation and net heat flux, and upwelling of warm waters in conditions of negative wind stress curl. Passage of a deep storm in the southern Weddell Sea on 6 November gave record strengthening of westerly winds that reduced the sea ice concentration triggering a progressive ice decline. The EIF formed on 8 December and grew rapidly reaching its maximum extent of 5.4×10^5 km^2 on 26 December, contributing significantly to the 1981 Weddell Sea sea ice extent minimum of 0.793×10^6 km^2, which was the lowest on record. The EIF developed differently than the 1970's Weddell Sea open ocean polynya, which formed within the winter sea ice cover due to enhanced deep reaching ocean convection. Investigating the impact of changes in the atmosphere and ocean on sea ice and the formation of polynyas in a warming climate is extremely important. A decrease in polynya events occurs with a weakening of convective activity[35] and increasing patterns are expected with the warming of subsurface water mass in the Southern Ocean[36]. Satellite observations show that the Weddell and Maud Rise polynyas reoccurred frequently after 2016 with a background of anomalously large decline in the Antarctic sea ice. As atmospheric and oceanic conditions become more extreme, more observational and modelling studies are required to examine

the long-term changes in the occurrence and intensity of polynyas. Obtaining more high-quality ocean data, along with in situ and satellite-based measurements of sea ice thickness is also important in improving our understanding of sea ice dynamics. We also need better ocean reanalyses, which have great potential to aid future polynya studies. More research is required to determine the influence of large ice-free features such as occurred in 1980 on the ocean and the sea ice conditions in the following years. Sensitivity experiments are also needed using ocean-ice-atmospheric models to quantify the relative contribution of various physical processes triggering the formation of polynyas in the central Weddell Sea and determine why the December 1980 EIF has not reappeared.

Methods

Sea ice observations

Daily (5-day trailing mean), monthly, and annual sea ice data based on passive microwave satellite observations were acquired from the US National Snow and Ice Data Centre sea ice index[37] (https://nsidc.org/). The conversion of satellite measurements into SIC can be applied via a number of different algorithms. The Fetterer SIC data were generated using the NASA Team algorithm 1.1 and cover late 1978 to the present. SIE was calculated as the total area of pixels where SIC was or exceeded 15%, whilst sea ice area (SIA) was calculated as the average SIC of a region multiplied by the size of the area. Several authors have used a threshold of SIC based upon 15% to 30% sea ice edge criteria for computing the SIE and SIA[15,25,38,39]. A threshold of 15% indicates a complete opening of the polynya. However, we have considered a higher threshold of 30% to calculate the size of extensive ice-free feature (EIF) which reflects the dynamic mix of open water and new ice. We took the Weddell Sea sector of the Southern Ocean to be the region bounded by 60 °W–20 °E (Fig. 1). No sea ice thickness data were available for 1980 as this pre-dated the routine operation of altimeters on polar orbiting satellites.

Atmospheric and ocean reanalysis

To determine the atmospheric conditions prior to the opening of the EIF we use the surface and upper air fields from the European Centre for Medium-range Weather Forecasts (ECMWF) fifth generation reanalysis (ERA5)[40] (https://www.ecmwf.int/en/forecasts/datasets/reanalysis-datasets/era5). We made use of mean sea level pressure (MSLP), near-surface temperature, wind, radiative flux (shortwave and longwave radiation), turbulent heat flux (sensible and latent heat) data. The net heat flux was computed after summing the radiative and turbulent heat flux variables. Hourly data were available with a ~ 31 km grid spacing. We focussed particularly on the latitude/longitude area 65°-70°S, 45°-30°W (which we refer to as the 'EIF box', Fig. 1), which broadly covers the area of the EIF at its maximum extent on 26 December 1980 (Fig. 1d). Ocean conditions were investigated using data from ECMWF's advanced operational ocean reanalysis system (ORAS5), which provides a near-surface vertical resolution of 1 m (https://www.ecmwf.int/en/forecasts/dataset/ocean-reanalysis-system-5). The depth where the potential density changes by 0.01 kg m^{-3} with reference to the surface was defined as the mixed layer depth. All anomalies were calculated against the 30-year base period 1980–2009.

Data availability

The ERA5 hourly fields are available from the Copernicus Climate Data Store, https://doi.org/10.24381/cds.bd0915c6. The ORAS5 ocean reanalysis data were obtained from https://www.ecmwf.int/en/forecasts/dataset/ocean-reanalysis-system-5. Sea ice extent and area data are available from the U.S. National Snow and Ice Data Center via https://nsidc.org/arcticseaicenews/sea-ice-tools/. Specific files used include S_Sea_Ice_Index_Regional_Daily_Data_G02135_v3.0 and S_Sea_Ice_Index_Regional_Monthly_Data_G02135_v3.0 for the regional daily and monthly data respectively. The Antarctic-wide monthly and annual data was obtained from Sea_Ice_Index_Monthly_Data_by_Year_G02135_v3.0. The majority of the datasets used in this study are available freely and the links are provided in the 'Methods' section above.

Code availability

All code used in this study is available on request from the corresponding author.

Received: 28 August 2023; Accepted: 17 June 2024;
Published online: 29 June 2024

References

1. Carsey, F. D. Microwave observations of the Weddell polynya. *Mon. Weather Rev.* **108**, 2032–2044 (1980).
2. Comiso, J. C. & Gordon, A. L. Cosmonaut polynya in the Southern Ocean: Structure and variability. *J. Geophys. Res. Ocean.* **101**, 18297–18313 (1996).
3. Francis, D., Eayrs, C., Cuesta, J. & Holland, D. Polar cyclones at the origin of the reoccurrence of the maud rise polynya in austral winter 2017. *J. Geophys. Res. Atmos.* **124**, 5251–5267 (2019).
4. Hirabara, M., Tsujino, H., Nakano, H. & Yamanaka, G. Formation mechanism of the Weddell Sea Polynya and the impact on the global abyssal ocean. *J. Oceanogr.* **68**, 771–796 (2012).
5. Ackley, S. F., Geiger, C. A., King, J. C., Hunke, E. C. & Comiso, J. The Ronne polynya of 1997/98: observations of air-ice-ocean interaction. *Ann. Glaciol.* **33**, 425–429 (2001).
6. Cheon, W. G. & Gordon, A. L. Open-ocean polynyas and deep convection in the Southern Ocean. *Sci. Rep.* **9**, 6935 (2019).
7. Martin, S. Polynyas. in *Encyclopedia of Ocean Sciences* 3rd edn (eds. Cochran, J. K., Bokuniewicz, H. J. & Yager, P. L) 175–180 (Academic Press, Oxford, 2019). https://doi.org/10.1016/B978-0-12-409548-9.11477-0.
8. Lee, Y. et al. *Causality and Evolution of Summer Polynyas off the Coast of Northern Greenland*. (EGU General Assembly 2020). https://doi.org/10.5194/egusphere-egu2020-6076.
9. Moore, G. W. K. & Pickart, R. S. The Wrangel Island Polynya in early summer: Trends and relationships to other polynyas and the Beaufort Sea High. *Geophys. Res. Lett.* **39**, 2011GL050691 (2012).
10. Schneider, W. & Budéus, G. Summary of the Northeast Water Polynya formation and development (Greenland sea). *J. Mar. Syst.* **10**, 107–122 (1997).
11. Fichefet, T. & Goosse, H. A numerical investigation of the spring Ross Sea polynya. *Geophys. Res. Lett.* **26**, 1015–1018 (1999).
12. Gordon, A. L. Oceanography: Southern Ocean polynya. *Nat. Clim. Chang.* **4**, 249–250 (2014).
13. Morales Maqueda, M. A., Willmott, A. J. & Biggs, N. R. T. Polynya dynamics: a review of observations and modeling. *Rev. Geophys.* **42**, 2002RG000116 (2004).
14. Turner, J. et al. Recent decrease of summer sea ice in the Weddell Sea, Antarctica. *Geophys. Res. Lett.* **47**, e2020GL087127 (2020).
15. Turner, J. et al. Record low antarctic sea ice cover in february 2022. *Geophys. Res. Lett.* **49**, e2022GL098904 (2022).
16. Holland, P. R. The seasonality of Antarctic sea ice trends. *Geophys. Res. Lett.* **41**, 4230–4237 (2014).
17. Jena, B., Ravichandran, M. & Turner, J. Recent reoccurrence of large open-ocean polynya on the maud rise seamount. *Geophys. Res. Lett.* **46**, 4320–4329 (2019).
18. Renfrew, I. A., King, J. C. & Markus, T. Coastal polynyas in the southern Weddell Sea: Variability of the surface energy budget. *J. Geophys. Res. Ocean.* **107**, 16–22 (2002).
19. Qin, Q., Wang, Z., Liu, C. & Cheng, C. Open-ocean polynyas in the cooperation sea, Antarctica. *J. Phys. Oceanogr.* **52**, 1363–1381 (2022).
20. Anderson, P. S. Evidence for an Antarctic winter coastal polynya. *Antarct. Sci.* **5**, 221–226 (1993).
21. Pease, C. H. The size of wind-driven coastal polynyas. *J. Geophys. Res. Ocean.* **92**, 7049–7059 (1987).

22. Campbell, E. C. et al. Antarctic offshore polynyas linked to Southern Hemisphere climate anomalies. *Nature* **570**, 319–325 (2019).
23. Francis, D., Mattingly, K. S., Temimi, M., Massom, R. & Heil, P. On the crucial role of atmospheric rivers in the two major Weddell Polynya events in 1973 and 2017 in Antarctica. *Sci. Adv.* **6**, eabc2695 (2020).
24. Yuan, X. & Li, C. Climate modes in southern high latitudes and their impacts on Antarctic sea ice. *J. Geophys. Res. Ocean.* **113**, 1–13 (2008).
25. Yuan, X. & Martinson, D. G. Antarctic sea ice extent variability and its global connectivity. *J. Clim.* **13**, 1697–1717 (2000).
26. Jena, B. et al. Mechanisms associated with the rapid decline in sea ice cover around a stranded ship in the Lazarev Sea, Antarctica. *Sci. Total Environ.* **821**, 153379 (2022).
27. Dufour, C. O. et al. Preconditioning of the Weddell Sea Polynya by the ocean mesoscale and dense water overflows. *J. Clim.* **30**, 7719–7737 (2017).
28. Cheon, W. G. et al. Replicating the 1970s' Weddell Polynya using a coupled ocean-sea ice model with reanalysis surface flux fields. *Geophys. Res. Lett.* **42**, 5411–5418 (2015).
29. Kumar, M. R. R. & Sadhuram, Y. Surface heat budget of a polynya in the coastal waters off Queen Maud Land, Antarctica, during austral summer. *Cont. Shelf Res.* **9**, 1063–1070 (1989).
30. Nihashi, S. & Ohshima, K. I. Relationship between ice decay and solar heating through open water in the Antarctic sea ice zone. *J. Geophys. Res. Ocean.* **106**, 16767–16782 (2001).
31. Nihashi, S. & Cavalieri, D. J. Observational evidence of a hemispheric-wide ice–ocean albedo feedback effect on Antarctic sea-ice decay. *J. Geophys. Res. Ocean*. **111**, 2005JC003447 (2006).
32. Ohshima, K. I., Nihashi, S. & Iwamoto, K. Global view of sea-ice production in polynyas and its linkage to dense/bottom water formation. *Geosci. Lett*. **3**, 13 (2016).
33. Gordon, A. L., Martinson, D. G. & Taylor, H. W. The wind-driven circulation in the Weddell-Enderby Basin. *Deep Sea Res. Part A. Oceanogr. Res. Pap.* **28**, 151–163 (1981).
34. Vernet, M. et al. The Weddell Gyre, southern ocean: Present knowledge and future challenges. *Rev. Geophys.* **57**, 623–708 (2019).
35. de Lavergne, C., Palter, J. B., Galbraith, E. D., Bernardello, R. & Marinov, I. Cessation of deep convection in the open Southern Ocean under anthropogenic climate change. *Nat. Clim. Chang.* **4**, 278 (2014).
36. Rheinlænder, J. W., Smedsrud, L. H. & Nisanciouglu, K. H. Internal ocean dynamics control the long-term evolution of Weddell Sea Polynya activity. *Front. Clim.* **3**, 1–17 (2021).
37. Fetterer, F., Knowles, K., Meier, W. N., Savoie, M. & Windnagel, A. K. *Sea Ice Index, Version 3 [Data Set]*. (National Snow and Ice Data Center, Boulder, Colorado USA, 2017) https://doi.org/10.7265/N5K072F8.
38. Bajish, C. C., Jena, B. & Anilkumar, N. Is the Indian monsoon rainfall linked to the Southern Ocean sea ice conditions? *Weather Clim. Extrem.* **34**, 100377 (2021).
39. Jena, B. et al. Record low sea ice extent in the Weddell Sea, Antarctica in April/May 2019 driven by intense and explosive polar cyclones. *npj Clim. Atmos. Sci.* **5**, 19 (2022).
40. Hersbach, H. et al. The ERA5 global reanalysis. *Q. J. R. Meteorol. Soc.* **146**, 1999–2049 (2020).

Acknowledgements

B.J. and C.C.B. express their gratitude to the Director, National Centre for Polar and Ocean Research, Group Director, Polar Science Group, and the Ministry of Earth Sciences, Government of India, for providing the essential facility and funding support. This support facilitated collaboration with the British Antarctic Survey through the DEFIANT project and the 'ObsSea4Clim–Ocean Observations and Indicators for Climate and Assessments' project under Horizon 2020. ObsSea4Clim, funded by the European Union (GA 101136548), is listed as contribution number 6. J.T. and C.H. received funding under NERC large grant DEFIANT NE/W004747/1. ZW was funded by the project supported by the Independent Research Foundation of Southern Marine Science and Engineering Guangdong Laboratory (Zhuhai) (SML2023SP201,313022009). We are grateful to NSIDC for the provision of the sea ice data and to ECMWF for the ERA5 fields. This work contains modified Copernicus Climate Change Service information 2021. Neither the European Commission nor ECMWF is responsible for any use that may be made of the Copernicus information or data it contains. The dataset Hersbach [2020] was downloaded from the Copernicus Climate Change Service (C3S) Climate Data Store. This is NCPOR contribution number J-8/2024-25.

Author contributions

B.J. and J.T. wrote the manuscript. All authors, including B.J., J.T., T.R.F., C.C.B., C.H., T.C.H., T.P. and Z.W., contributed to the analyses, interpretation of results, and revision of the manuscripts.

Competing interests

The authors declare no competing interests.

Additional information

Supplementary information The online version contains supplementary material available at https://doi.org/10.1038/s41612-024-00700-7.

Correspondence and requests for materials should be addressed to Babula Jena.